Manganese deficiency alters photosynthetic electron transport in Marchantia polymorpha

Umama Hani, Anja Krieger-Liszkay

Plant Physiology and Biochemistry 215 (2024) 109042

Contents lists available at ScienceDirect

Plant Physiology and Biochemistry

journal homepage: www.elsevier.com/locate/plaphy

Manganese deficiency alters photosynthetic electron transport in *Marchantia polymorpha*

Umama Hani, Anja Krieger-Liszkay *

Université Paris-Saclay, Institute for Integrative Biology of the Cell (I2BC), CEA, CNRS, 91198, Gif-sur-Yvette cedex, France

ARTICLE INFO

Handling Editor: Dr. Mario De Tullio

Keywords:
Cyclic electron transport
In vivo absorption spectroscopy
Marchantia polymorpha
Photosystem I
Plastocyanin

ABSTRACT

Manganese (Mn) is considered as an essential element for plant growth. Mn starvation has been shown to affect photosystem II, the site of the Mn_4CaO_5 cluster responsible for water oxidation. Less is known on the effect of Mn starvation on photosystem I. Here we studied the effects of Mn deficiency *in vivo* on redox changes of P700 and plastocyanin (Pc) in the liverwort *Marchantia polymorpha* using the KLAS-NIR spectrophotometer. Far-red illumination is used to excite preferentially photosystem I, thus facilitating cyclic electron transport. Under Mn starvation, we observed slower oxidation of P700 and a decrease in the Pc signal relative to P700. The lower Pc content under Mn deficiency was confirmed by western blots. Re-reduction kinetics of $P700^+$ and Pc^+ were faster in Mn deficient thalli than in the control. The above findings show that the kinetics studied under Mn deficiency not only depend on the number of available reductants but also on how quickly electrons are transferred from stromal donors via the intersystem chain to Pc^+ and $P700^+$. We suggest that under Mn deficiency a structural reorganization of the thylakoid membrane takes place favoring the formation of supercomplexes between ferredoxin, cytochrome b_6f complex, Pc and photosystem I, and thus an enhanced cyclic electron transport.

1. Introduction

Manganese (Mn) is one of the essential trace elements for plant growth and development. Mn is known as an indispensable constitutive element of the Mn_4O_5Ca cluster in photosystem II (PSII), where it oxidizes water molecules and thus provides the necessary electrons for oxygenic photosynthesis (Shen, 2015; Alejandro et al., 2020). Plants require an optimal supply of Mn to maintain homeostatic balance (Alejandro et al., 2020). Besides its role in PSII, Mn has an important role as co-factor of various enzymes including catalase (MnCAT), superoxide dismutase (MnSOD), decarboxylases of tricarboxylic acid (TCA) cycle (Marschner, 2011; Corpas et al., 2017) and in other metabolic processes (Schmidt et al., 2016; Bhat et al., 2020). Mn deficiency strongly impacts photosynthesis, mainly PSII, accompanied by subtle perturbation in chloroplast ultrastructure (Papadakis et al., 2007; Messant et al., 2023). Initial signs of Mn deficiency typically appear first in younger leaves, which includes paleness accompanied by interveinal chlorosis (Schmidt et al., 2016). However, symptoms of Mn deficiency vary depending on the species (Homann, 1967).

Contrary to the research done on effects of Mn deficiency on PSII, very limited information concerning its consequences on PSI is available. We have previously studied the effects of Mn excess and deficiency in liverwort *Marchantia polymorpha*, for which we established the conditions for Mn concentration for optimal growth and a condition to induce Mn deficiency (Messant et al., 2023). With well-explored taxonomy and morphology, *M. polymorpha* stands as a complex thalloid liverwort (Bowman, 2016), residing mainly at the marginal area between aquatic and land environments. Today's use of *M. polymorpha* as a model plant is primarily based on its genomic simplicity (Bowman et al., 2016; Bowman, 2022) and ease of propagation (Naramoto et al., 2022). In our recent study, we investigated the effect of Mn deficiency on photosynthesis in *M. polymorpha*. Under Mn starvation, a change in the ratio of PSI/PSII capacities was observed. Moreover, we also showed changes in structural organization of thylakoid membrane. Most importantly for the present study, less limitation of electron donation to $P700^+$ in actinic light was observed under Mn deficiency. We interpreted the difference in stoichiometry of PSI/PSII and the lower donor-side limitation of PSI as an increase in cyclic electron transport (CET) under Mn starvation (Messant et al., 2023). CET is one of the alternative electron pathways that comes into play under certain physiological conditions, especially upon stress (Sunil et al., 2019) with the main aim of balancing the ATP/NADPH ratio. CET involves cycling of

* Corresponding author.
E-mail address: anja.liszkay@i2bc.paris-saclay.fr (A. Krieger-Liszkay).

https://doi.org/10.1016/j.plaphy.2024.109042
Received 29 March 2024; Received in revised form 7 August 2024; Accepted 11 August 2024
Available online 16 August 2024

electrons around PSI, generating a proton gradient and thereby ATP without generating NADPH (for recent reviews see e.g., Nawrocki et al., 2019; Takahashi, 2022).

The current study aims to further explore the effects of Mn deficiency on PSI in *M. polymorpha*, with the main objective of investigating changes in oxido-reduction of P700 and plastocyanin (Pc) using KLAS-NIR spectrophotometer. KLAS-NIR is a pulse-amplitude modulation spectrophotometer that has been developed by Klughammer and Schreiber (2016) to study deconvoluted signals in the near infra-red of P700 and Pc *in vivo*, i.e. in thalli in our case. We particularly have chosen the approach of inducing CET by irradiating thalli with far-red (FR) light, thus facilitating the measurement of CET. FR light is preferentially absorbed by PSI and maximally oxidizes P700 to the extent of 80–90% (Chow et al., 2012; Pettai et al., 2005).

2. Materials and methods

2.1. Plant material

Gemmae from Takaragaike (Tak-1) male accession of *M. polymorpha* were cultured for two weeks under a light-dark cycle (16 h light, 22 °C, 100 μmol photons $m^{-2}s^{-1}$, white fluorescent lamp; 8 h-dark, 20 °C) on one-half-strength Gamborg's B5 media (GB5) with 1% Agar (Gamborg et al., 1968). To create Mn deficiency, thalli were transferred to ½ GB5 media containing 6% starch with or without addition of 33 μM $MnCl_2$ for a week prior to performing desired experiments (Messant et al., 2023).

2.2. Thylakoids isolation and immunoblots

Thalli from three-weeks old *M. polymorpha* were harvested and after careful washing with water to remove starch, were grounded in a buffer containing 0.33 M sorbitol, 1 mM EDTA, 1 mM $MgCl_2$, 50 mM KCl, 25 mM MES-KOH (pH 6.1). The resulting slurry was filtered through two layers of cheese cloth and one layer of miracloth. After centrifugation, the pellet was re-suspended in 25 mM HEPES-KOH (pH 6.7), 0.33 M sorbitol, 1 mM EDTA, 1 mM $MgCl_2$, 50 mM KCl and washed twice. Finally, the isolated thylakoids were re-suspended and stored in 25 mM HEPES-KOH (pH 7.6), 0.33 M sorbitol, 1 mM $MgCl_2$, 50 mM KCl. All centrifugation steps were performed at 3,000×*g* for 3 min at 4 °C. Chlorophyll content was measured according to Arnon (1949).

For immunodetection, proteins from the thylakoids extract were separated using 12% (w/v) sodium dodecyl polyacrylamide gel electrophoresis (SDS-PAGE). After electrophoresis, proteins were transferred to nitrocellulose membrane (Amersham™ Protran, 0.45 μm pore size) and incubated with primary antibodies (Pc, PsaC, PetB and cytb_{559}) at room temperature in TBS-T (0.1 % Tween-20 (v/v), containing 5% non-fat milk powder). After washing with TBS-T, the membranes were decorated with anti-rabbit peroxidase-linked secondary antibodies. Bands were visualized with enhanced chemiluminescence (ChemiDoc™ Touch Imaging System, Bio-Rad) after 1–2 min incubation with ECL solution (Amersham ECL Prime Western Blotting Detection Reagent). Antibodies directed against Pc (AS06 141), PsaC (AS10 939), PetB (AS18 4169) were purchased from Agrisera (Vännäs, Sweden), antibodies directed against cytb_{559} were kindly provided by P. Beyer, Freiburg University, Germany. Densitometric analysis of blots was performed with image J (https://imagej.nih.gov/ij/).

2.3. RT-PCR

Plant Mini RNeasy kit (Qiagen, Venlo, Netherlands) was used for total RNA extraction, and samples were homogenized with RLT lysis buffer. RT reactions were done with the SuperScript IV Reverse Transcriptase kit (Invitrogen, Carlsbad, USA). cDNA was diluted 4 times with LightCycler 480 SYBR Green I Master (Roche, Penzberg, Germany) reaction medium (1X final concentration) containing 2.5 μM of each primer (Table S1). The mRNA levels of plastocyanin (Mp4g02720.1_Sequence extracted from "MarpolBase"; genome database for *Marchantia*) were normalized to reference housekeeping gene ACTIN 1 (*MpACT1*: Mp6g10990).

2.4. Chlorophyll fluorescence and P700 measurements

Chlorophyll fluorescence and P700 absorbance were measured using a Dual-PAM-100 fluorometer (Walz, Effeltrich, Germany). Effective quantum yield of PSII: Y(II) = (Fm'-F)/Fm' and non-photochemical quenching: qN=(Fm–Fm')/Fm, were measured as a function of light intensity. Each actinic light intensity was applied for 180 s. For P700 measurements, dark adapted thalli were exposed to three different actinic light intensities (64, 175 and 803 μmol quanta $m^{-2}s^{-1}$) and far-red light followed by a saturating flash at the end of far-red light period.

2.5. KLAS-NIR measurements

All the measurements were made with kinetic-LED-array-spectrophotometer (KLAS) (Walz, Effeltrich, Germany) that utilizes pulse amplitude modulation within the NIR-Infrared (NIR) spectral range and operates in the dual-wavelength difference mode (785–840, 810–870, 870–970 and 795–970 nm) (Schreiber and Klughammer, 2016; Schreiber, 2017). Technical details of the KLAS-NIR spectrophotometer and the principle behind the deconvolution of P700, Pc and Fd are explained in detail by Klughammer and Schreiber (2016). All measurements were done under "Slow kinetics window". Transmittance changes were recorded with high-resolution trigger run file called "NIR max" along with data acquisition every ms (Fig. 2). Kinetics recording and illumination steps were fully automated. NIR max protocol includes three main components. After dark adaptation, the sample was illuminated with Actinic Light (AL10, 572 μmol quanta $m^{-2}s^{-1}$) for 3 s and 30 ms pulse of light at saturating light intensity (6500 μmol quanta $m^{-2}s^{-1}$) was applied during illumination with AL. The second component involves switching on the FR light (FR18) for 10 s that lead to almost maximal oxidation of P700 and Pc. At the end, a 300 ms saturating flash was given to fully induce oxidation of P700 and Pc (P700 and Pc MAX values). Kinetics of P700 oxidation (Fig. 4) and $P700^+$ and Pc^+ re-reduction (Figs. 5 and 6) were studied with FR-on (FR10) and FR-off respectively.

2.6. Transmission electron microscopy

About 1 mm strips of thalli were cut and fixed with glutaraldehyde/paraformaldehyde fixative and later infused with 1% osmium (w/v) and 1.5% potassium hexacyanoferrate (w/v) en bloc staining protocol as described (Hawes et al., 1981; Juniper et al., 1982); EM UC6 ultramicrotome (Leica microsystems) was used for cutting 70 mm thick sections to be deposited on to copper grids. Ultrathin sections were stained with 2% uranyl acetate (w/v) (Merck) and Reynolds lead citrate according to standard procedures. Grids were examined under a JEOL 1400 TEM operating at 80 kV (JEOL, http://www.jeol.com). Images were acquired using a 9-megapixel high-speed camera (RIO9; Gatan, http://www.gatan.com) and processed using Digital Micrograph (Gatan).

3. Results

In the current study, we aimed to investigate the effect of Mn deficiency on photosynthetic electron transport in *M. polymorpha* in more detail compared with the study by Messant et al. (2023). Fig. 1 shows that Y(II) was lower and qN was higher in Mn-deficient thalli than in thalli grown in control conditions. In addition to PSII, P700 oxidation is also affected under Mn deficiency. At light intensities higher than growth light, P700 oxidation was slower and a lower steady state oxidation level was reached at an actinic red light intensity of 175 μmol quanta $m^{-2}s^{-1}$. We have reported previously that limitation of electron donation to PSI was lower in Mn-deficient thalli than in thalli grown in

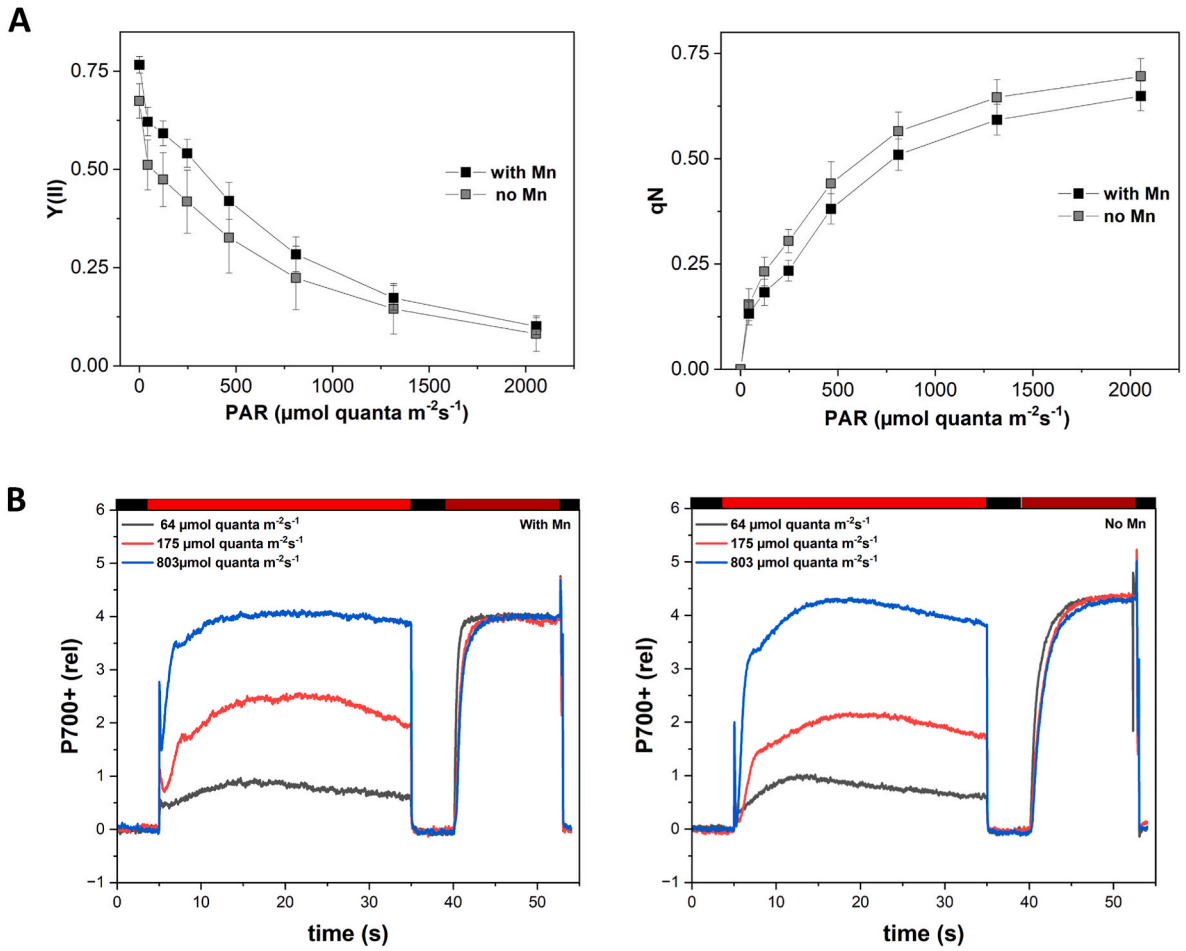

Fig. 1. Chlorophyll fluorescence and P700 measurements in response to different light intensities in *Marchantia* thalli grown in control and Mn-deficient conditions. Effective quantum yield of PSII (YII) and non-photochemical quenching (qN) measured as function of light intensity. Data are represented as the mean ± SD of 5 biological replicates (A). For P700 oxidation measurements, red actinic light (803, 175 and 64 µmol quanta $m^{-2}s^{-1}$) and far-red light were given as indicated in the coloured bars. To get the maximum oxidation amplitude of P700, a saturation flash was given at the end of the far-red illumination. Measurements with three independent biological replicates were performed and representative traces are shown (B).

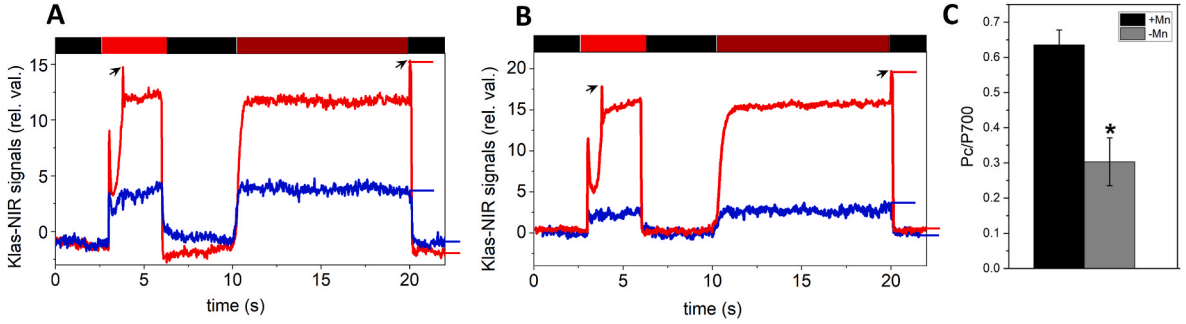

Fig. 2. Redox changes in P700 and Plastocyanin in *Marchantia* thalli grown in control and Mn-deficient conditions. Changes in the redox states of P700 (red) and plastocyanin (Pc; blue) in thalli grown in control conditions (+Mn; **A**) and in Mn-deficiency (-Mn**; B**) upon illumination with red actinic light (570 µmol quanta $m^{-2}s^{-1}$) and far-red light. Saturation flashes were applied at 4 s and 20 s as indicated by black arrows. Horizontal marks indicate the maximum intensity levels (under far-red light) and the zero levels (in the dark) for P700 and Pc. Top of the figure indicates the illumination protocol (red = Actinic light, dark red = Far-red light). Figures A, B show representative traces. The mean absorption values of the calculated ratio (Pc/P700) for + Mn and –Mn are given in **C**, 3 independently grown biological replicates, n = 9. Statistically significance (*$P < 0.05$) was assessed by Student's *t*-test.

control conditions while the capacity of PSII electron transport was lowered (Messant et al., 2023). To study oxidation of P700 and Pc in parallel, we used the KLAS NIR spectrophotometer. The kinetics shown in Fig. 2 were obtained using the "NIR-Max" protocol of KLAS NIR spectrophotometer. Changes in the redox states of P700 and Pc in response to red-actinic and far-red light are shown for 3-weeks old thalli of *Marchantia polymorpha*. The maximum oxidation levels for P700 and Pc were determined through a saturation flash following the far-red light. Calculated "relative" values indicate the amount of photo-oxidized (and reduced) P700 and Pc. Compared with $P700^{+}$

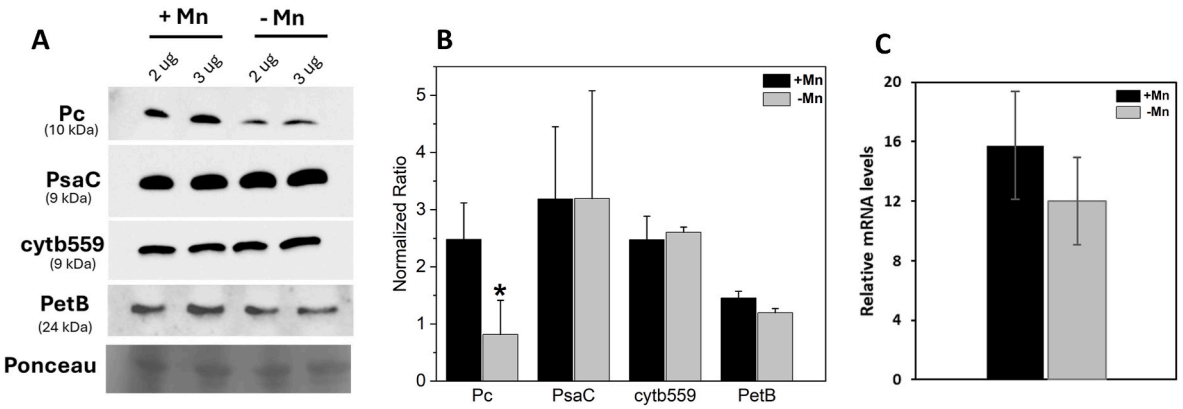

Fig. 3. Western blots and RT-PCR analysis of plastocyanin in *Marchantia* grown in control and Mn-deficient conditions. Representative immunoblots showing the content of Pc (Plastocyanin), PsaC (PSI subunit),cytb_{559} (PSII subunit) and PetB (cyt b_6f subunit) in thylakoids extracted from *Marchantia polymorpha*, grown in the presence of Mn (+Mn) and under Mn deficiency (-Mn). Gels were loaded based on chlorophyll content and ponceau red staining is shown as loading control (**A**). Densitometric analysis (**B**), mean value ± SE of three to six biological replicates are shown. Statistically significance (*P < 0.05) was assessed by Student's *t*-test. RT-PCR data for Pc (mean value ± SE) of two biological replicates are shown (C).

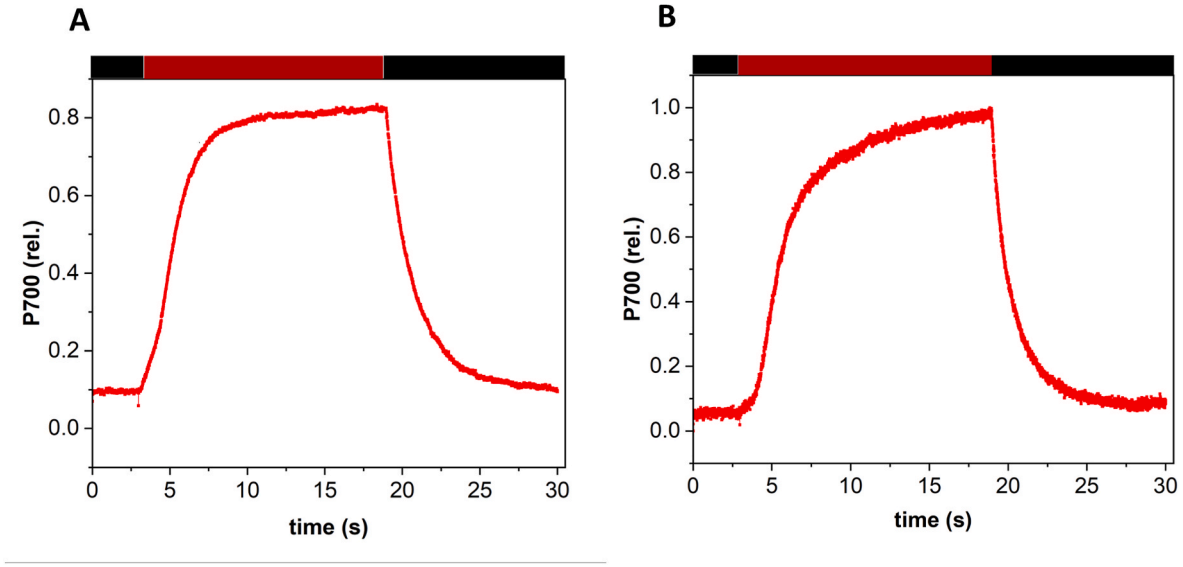

Fig. 4. Far-red light (FR) illumination shows differences in the kinetics of P700 oxidation in Mn-deficient samples. Thalli grown in control (A) and Mn-deficient (B) conditions were illuminated with FR light for 15 s. Top of the figure indicates the illumination protocol. The representative curves shown are an average of 10 traces. In total, 3 biological replicates were measured, each with 2 technical replicates.

amplitude, in far-red light, the amplitude of Pc oxidation was significantly smaller (≤50 %) under Mn deficiency (Fig. 2B) than in the presence of Mn (Fig. 2A). Fig. 2C shows significant changes for the calculated Pc to P700 ratio. The decrease in Pc content was confirmed by immunoblotting using specific antibodies. A clear decrease in the Pc content was visible under Mn deficiency (Fig. 3A), while PsaC (PSI subunit), cytb_{559} (PSII subunit) and PetB (cyt b_6f subunit) remained stable under both conditions. RT-PCR analysis of Pc (Fig. 3C) showed no significant differences between the two growth condition, indicating that it is not the expression levels but rather the protein stability that is responsible for the low Pc content under Mn deficiency.

The question arises how a low content of Pc affects electron donation to $P700^+$. We reported earlier lower donor-side limitation in Mn-deficient *Marchantia* when illuminated with red actinic light. Fig. 4 shows P700 oxidation kinetics induced by far-red light of dark-adapted *Marchantia* thalli. A considerable difference in P700 oxidation was noticed between control (+Mn) and Mn-deficient (-Mn) samples. In the presence of Mn (Fig. 4A), far red light triggered P700 oxidation within 8s, whereas under Mn deficiency (Fig. 4B) P700 is oxidized more slowly, indicating that more electrons are available to be donated to $P700^+$, thereby delaying the time until maximum $P700^+$ accumulation is observed. This slow rise of P700 oxidation may indicate a higher cyclic electron transport.

To further see the effect of Mn deficiency on PSI, reduction of $P700^+$ was studied after turning off the far-red light. Fig. 5 shows a significantly slower re-reduction of $P700^+$ under control conditions than under Mn deficiency. Half times ($t_{1/2}$) of $P700^+$ were determined as 3.7 s ± 0.01 and 1.9 s ± 0.007 for + Mn and -Mn, respectively. The faster re-reduction of $P700^+$ indicates again that more electrons are available to be donated to $P700^+$, suggesting a higher CET or less strong photosynthetic control under Mn deficiency. Moreover, we also reported faster re-reduction of Pc^+ in Mn-deficient thalli than in control thalli (Fig. 6). Pc^+ reduction was about 2.5-fold slower in comparison with $P700^+$. In the presence of the uncoupler nigericin the opposite effect was observed (Fig. S1). Both, the $t_{1/2}$ for $P700^+$ reduction and for Pc^+ reduction were slower under Mn deficiency than in control conditions. This shows that in the presence of nigericin under Mn deficiency less electron donors are available to reduce $P700^+$ and Pc^+.

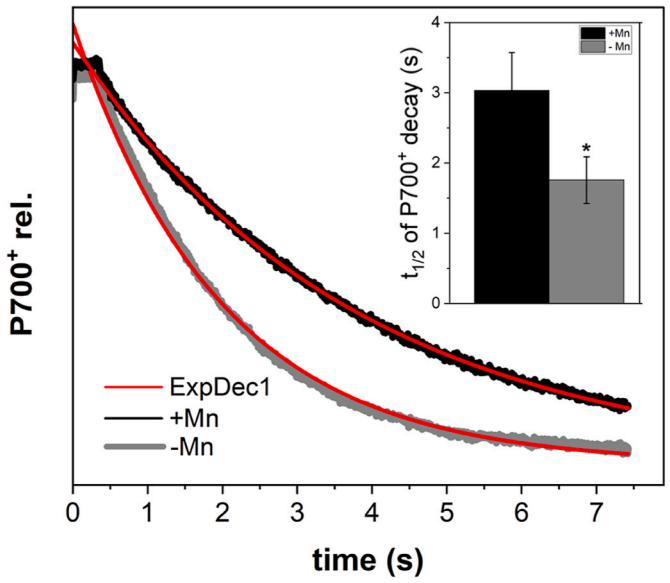

Fig. 5. Re-reduction kinetics of P700$^+$ after FR illumination. The kinetics of P700$^+$ re-reduction in Marchantia thalli indicated in black and grey for + Mn and –Mn, respectively, were monitored in the dark, after 5s exposure to FR light. Decay signals for P700$^+$ were fitted with single exponential function (red traces). The curves represent an average of 6 measurements for each sample. The inset show the half times ($t_{1/2}$) calculated for P700$^+$ decay (samples from three independent cultures, n = 6). Statistical significance (*P < 0.05) was assessed by Student's *t*-test.

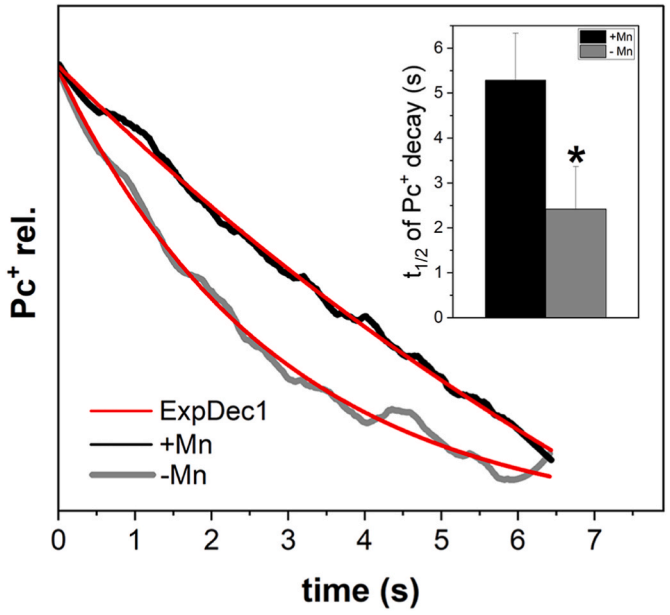

Fig. 6. Re-reduction kinetics of Pc$^+$ after FR illumination. The kinetics of Pc$^+$ re-reduction in *Marchantia* thalli indicated as black and grey for + Mn and –Mn respectively, were monitored in the dark, after 5s exposure to FR light. Decay signals for P700$^+$ were fitted with single exponential function (red traces). The curves represent an average of 6 measurements for each sample. The inset show the half times ($t_{1/2}$) calculated for Pc$^+$ decay (samples from three independent cultures, n = 6). Statistical significance (*P < 0.05) was assessed by Student's *t*-test.

4. Discussion

Here, we studied transient absorption changes in P700 and Pc using the KLAS-NIR spectrophotometer in the liverwort *M. polymorpha* grown in control and Mn-deficient conditions. According to the maximum signals for Pc$^+$ (Fig. 2) and immunoblot analysis (Fig. 3), the Pc signal relative to the P700 signal is drastically decreased upon Mn deficiency (Fig. 2). In *Arabidopsis*, it has been shown that the Pc content can be significantly decreased without pronounced changes in the overall photosynthetic activity, suggesting that Pc is present in large excess under control growth conditions (Pesaresi et al., 2009). However, in tobacco Schöttler et al. (2004) observed a reduction of electron transport and assimilation capacity when the amount of Pc was decreased. A decrease in Pc content has previously also been reported in early stages of senescence in tobacco and barley (Schöttler et al., 2004; Shimakawa et al., 2020). In Marchantia, lower Pc content induced by Mn deprivation, affects electron donation to PSI. The slower rate of P700 oxidation upon illumination of dark-adapted sample with red and FR light under Mn deficiency (Fig. 2B and 4B, see also Fig. 7 in Messant et al., 2023) and the faster re-reduction of P700$^+$ (Fig. 5) and Pc$^+$ (Fig. 6), show that either more electron donors are available for the reduction of these compounds, or that the electron transport becomes faster. Extra electron donation could originate from enhanced chlororespiration; lower photosynthetic control or from enhanced cyclic electron transport under Mn deficiency. Since lower donor-side limitation is also observed upon illuminations with actinic red light, a condition that outcompetes the chlororespiration pathway, we suggest that either less strong photosynthetic control or more cyclic electron transport is taking place under Mn deficiency than under control conditions. In Figs. 4–6, we have studied the effect of FR illumination. FR light excites preferentially PSI and cyclic electron transport is favored compared with red light illumination (Heber et al., 1978). In KLAS-NIR, using FR light at 720 nm, in a leaf the quantum yield of PSII of absorbed light is about 15% compared with illumination at 620 nm (Pettai et al., 2005). This low PSII activity is sufficient to supply electrons at a low rate via linear electron flow to sustain cyclic flow. After illumination with FR light, the re-reduction kinetics of P700$^+$ takes place with a $t_{1/2}$ of 3.7 s ± 0.01 in control and 1.9 s ± 0.007 in Mn-deficient samples (Fig. 5). These kinetics are rather slow compared to the kinetics observed after illumination with red actinic light in higher plants (see for example Shimakawa et al., 2020). However, comparable half-time of 1.7 s for PSI CET has been previously reported for *Arabidopsis thaliana* (Jensen et al., 2000). The faster reduction of P700$^+$ and Pc$^+$ could also be explained by a lower photosynthetic control under Mn deficiency. Donor-side limitation to PSI is lower under Mn deficiency as we have reported earlier (Messant et al., 2023). This could be either caused by increased cyclic flow or lower photosynthetic control. qN was higher under Mn deficiency (Fig. 1), speaking for a larger proton gradient and, presumably, a higher photosynthetic control. When the thalli had been infiltrated with nigericin the reduction of P700$^+$ and Pc$^+$ was slower under Mn deficiency (Fig. S1), opposite to what has been observed in the absence of an uncoupler (Figs. 5 and 6). This observation could be explained by lower photosynthetic electron transport and lower NADPH production since the PSII activity is decreased under Mn deficiency (Fig. 1A, see also data in Messant et al., 2023).

A comparison between P700$^+$ and Pc$^+$ reduction kinetics shows that Pc$^+$ reduction is 2.5-fold slower than that of P700$^+$, both in control and under Mn deficiency. This can be explained by an amount of Pc larger than that of PSI reaction centers. Upon Mn deficiency, the ratio Pc/P700 decreased by about 50% while the reduction of P700$^+$ and Pc$^+$ was accelerated. The faster reduction of P700$^+$ and of Pc$^+$ under Mn deficiency shows clearly that the kinetics not only depend on the number of available reductants in stroma and Pc electron carriers in the lumen but also on how quickly electrons can transfer from the stromal donors via the intersystem chain to Pc$^+$ and from there to P700$^+$. It has been reported previously that a decrease in the amount of Pc limits electron transport on the donor side of PSI probably caused by the limitation of lateral diffusion of Pc between the cyt b_6f complex and PSI (Drepper et al., 1996; Haehnel, 1982; Cruz et al., 2001). In the present case, however, the electron transport is accelerated when the Pc pool is small.

Using the data shown in Fig. 2 and the extinction coefficient of P700 and Pc determined *in vitro* (Sétif et al., 2019), the molar ratio of Pc to P700 is about 1.6 in control and 0.8 under Mn starvation. Even if this determination is an underestimation of the Pc content, under Mn deficiency too few Pc would be available for maintaining efficient electron transport between cyt b_6f complex, Pc and PSI. This speaks for a structural reorganization of the complexes and the formation of supercomplexes formed between ferredoxin, cytb_6f complex, Pc and PSI. According to the study conducted by Joliot and Joliot (2002), PSI, cytb_6f complex, Fd and Ferredoxin $NADP^+$-reductase (FNR) are physically associated and serve as a platform for Fd-dependent CET, leading to slow leakage of electrons and ultimately limited photo-oxidation of P700. In the green alga *Chlamydomonas reinhardtii* supercomplexes composed of PSI, Pc, cytb_6f complex, Fd have been biochemically isolated (Iwai et al., 2010), and functional supercomplexes have been biophysically characterized (Joliot et al., 2022). Moreover, a low-resolution structure of a PSI-LHCI-cytb_6f complex has been also revealed in *C. reinhardtii* (Steinbeck et al., 2018). Alterations of the organization of the thylakoid membrane may favor the formation of such supercomplexes. According to transmission electron microscopy images (Fig. S2), the organization of the thylakoid membrane is affected by Mn deprivation. In *in vivo* super-resolution chlorophyll fluorescence emission microscopy strongly fluorescent regions were localized more distinctly in chloroplasts of Mn-deficient thalli, indicating a change in the mesoscopic organization of the thylakoid membrane (Messant et al., 2023). This indicates smaller grana stacks with a more pronounced segregation between them and the stroma lamellae.

Enhancement of cyclic electron transport upon abiotic stress conditions allows to generate a higher pmf and a higher ATP/NADPH ratio. CET is known to increase under certain stress conditions like drought, low CO_2, low N, low temperature, and heavy metal stress (for review, see Sunil et al., 2019). CET is crucial for protecting PSI by alleviating the over-reduction of the acceptor side of PSI. *Marchantia* possess flavodiiron proteins and over-reduction of the acceptor side of PSI is less critical than in angiosperms (Shimakawa et al., 2017), however, upon Mn deficiency the capacity of linear electron flow is diminished and maintaining a high ATP level may be physiologically important to survive photoautrophically. Future work is needed to show if CET is increased under deprivation of other micronutrients than Mn. In addition, the biochemical composition of the putative supercomplex involved in CET under Mn deficiency in *Marchantia* should be analyzed.

Author contribution

U. H., and A.K-L. designed the project. U.H. performed the experiments; U.H. and A.K-L. analyzed the data. U. H., and A.K-L. wrote the manuscript.

Funding

This work was supported by the Labex Saclay Plant Sciences-SPS (ANR-17-EUR-0007), the platform of Biophysics of the I2BC supported by the French Infrastructure for Integrated Structural Biology (FRISBI; grant number ANR-10-INSB-05), IBiSA and France-BioImaging infrastructure (ANR-10-INBS-04, call “investissements d’Avenir”). U.H. is supported by a CNRS PhD contract.

Declaration of competing interest

The authors declare the following financial interests/personal relationships which may be considered as potential competing interests: Anja Krieger-Liszkay reports financial support was provided by French National Research Agency. If there are other authors, they declare that they have no known competing financial interests or personal relationships that could have appeared to influence the work reported in this paper.

Data availability

Data will be made available on request.

Acknowledgements

We would like to thank Sébastien Thomine (I2BC) for hosting U.H. in his laboratory, Claire Boulogne (I2BC) for her help with electron microscopy and Ginga Shimakawa (Kobe university, Japan) for scientific discussions.

Appendix A. Supplementary data

Supplementary data to this article can be found online at https://doi.org/10.1016/j.plaphy.2024.109042.

References

Alejandro, S., Höller, S., Meier, B., Peiter, E., 2020. Manganese in plants: from acquisition to subcellular allocation. Front. Plant Sci. 11, 517877.
Arnon, D.I., 1949. Copper enzymes in isolated chloroplasts. Polyphenoloxidase in Beta vulgaris. Plant Physiol. 24 (1), 1.
Bhat, B.A., Islam, S.T., Ali, A., Sheikh, B.A., Tariq, L., Islam, S.U., Hassan Dar, T.U., 2020. Role of micronutrients in secondary metabolism of plants. Plant Micronutrients: Def. Toxic. Manag. 311–329.
Bowman, J.L., 2016. A brief history of Marchantia from Greece to genomics. Plant Cell Physiol. 57 (2), 210–229.
Bowman, J.L., 2022. The liverwort Marchantia polymorpha, a model for all ages. In: Current Topics in Developmental Biology, vol. 147. Academic Press, pp. 1–32.
Bowman, J.L., Araki, T., Arteaga-Vazquez, M.A., Berger, F., Dolan, L., Haseloff, J., et al., 2016. The naming of names: guidelines for gene nomenclature in Marchantia. Plant Cell Physiol. 57 (2), 257–261.
Chow, W.S., Fan, D.Y., Oguchi, R., Jia, H., Losciale, P., Park, Y.I., et al., 2012. Quantifying and monitoring functional photosystem II and the stoichiometry of the two photosystems in leaf segments: approaches and approximations. Photosynth. Res. 113, 63–74.
Corpas, F.J., Barroso, J.B., Palma, J.M., Rodriguez-Ruiz, M., 2017. Plant peroxisomes: a nitro-oxidative cocktail. Redox Biol. 11, 535–542.
Cruz, J.A., Salbilla, B.A., Kanazawa, A., Kramer, D.M., 2001. Inhibition of plastocyanin to P_{700}^+ electron transfer in Chlamydomonas reinhardtii by hyperosmotic stress. Plant Physiol. 127, 1167–1179.
Drepper, F., Hippler, M., Nitschke, W., Haehnel, W., 1996. Binding dynamics and electron transfer between plastocyanin and photosystem I. Biochemistry 35 (4), 1282–1295.
Gamborg, O.L., Miller, R., Ojima, K., 1968. Nutrient requirements of suspension cultures of soybean root cells. Exp. Cell Res. 50 (1), 151–158.
Haehnel, W., 1982. On the functional characterization of electron transport from plastoquinone to photosystem I. Biochim. Biophys. Acta 682, 245–257.
Hawes, C.1., Juniper, B.E., Horne, J.C., 1981. Low and high voltage electron microscopy of mitosis and cytokinesis in maize roots. Planta 152, 397–407.
Heber, U., Egneus, H., Hanck, U., Jensen, M., Köster, S., 1978. Regulation of photosynthetic electron transport and photophosphorylation in intact chloroplasts and leaves of Spinacia oleracea L. Planta 143 (1), 41–49.
Homann, P., 1967. Studies on the manganese of the chloroplast. Plant Physiol. 42 (7), 997–1007.
Iwai, M., Takizawa, K., Tokutsu, R., Okamuro, A., Takahashi, Y., Minagawa, J., 2010. Isolation of the elusive supercomplex that drives cyclic electron flow in photosynthesis. Nature 464 (7292), 1210–1213.
Jensen, P.E., Gilpin, M., Knoetzel, J., Scheller, H.V., 2000. The PSI-K subunit of photosystem I is involved in the interaction between light-harvesting complex I and the photosystem I reaction center core. J. Biol. Chem. 275 (32), 24701–24708.
Joliot, P., Sellés, J., Wollman, F.A., Verméglio, A., 2022. High efficient cyclic electron flow and functional supercomplexes in Chlamydomonas cells. Biochim. Biophys. Acta Bioenerg. 1863 (8), 148909.
Joliot, P., Joliot, A., 2002. Cyclic electron transfer in plant leaf. Proc. Natl. Acad. Sci. USA 99 (15), 10209–10214.
Juniper, B.E., Hawes, C.R., Horne, J.C., 1982. The relationships between the dictyosomes and the forms of endoplasmic reticulum in plant cells with different export programs. Bot. Gaz. 143 (2), 135–145.
Klughammer, C., Schreiber, U., 2016. Deconvolution of ferredoxin, plastocyanin, and P700 transmittance changes in intact leaves with a new type of kinetic LED array spectrophotometer. Photosynth. Res. 128, 195–214.
Marschner, H. (Ed.), 2011. Marschner’s Mineral Nutrition of Higher Plants. Academic press.
Messant, M., Hani, U., Hennebelle, T., Guérard, F., Gakière, B., Gall, A., et al., 2023. Manganese concentration affects chloroplast structure and the photosynthetic apparatus in Marchantia polymorpha. Plant Physiol. 192 (1), 356–369.
Naramoto, S., Hata, Y., Fujita, T., Kyozuka, J., 2022. The bryophytes Physcomitrium patens and Marchantia polymorpha as model systems for studying evolutionary cell and developmental biology in plants. Plant Cell 34 (1), 228–246.

Nawrocki, W.J., Bailleul, B., Picot, D., Cardol, P., Rappaport, F., Wollman, F.A., Joliot, P., 2019. The mechanism of cyclic electron flow. Biochim. Biophys. Acta Bioenerg. 1860 (5), 433–438.
Papadakis, I.E., Giannakoula, A., Therios, I.N., Bosabalidis, A.M., Moustakas, M., Nastou, A., 2007. Mn-induced changes in leaf structure and chloroplast ultrastructure of Citrus volkameriana (L.) plants. J. Plant Physiol. 164 (1), 100–103.
Pesaresi, P., Scharfenberg, M., Weigel, M., Granlund, I., Schröder, W.P., Finazzi, G., Rappaport, F., Masiero, S., Furini, A., Jahns, P., Leister, D., 2009. Mutants, overexpressors, and interactors of Arabidopsis plastocyanin isoforms: revised roles of plastocyanin in photosynthetic electron flow and thylakoid redox state. Mol. Plant 2 (2), 236–248.
Pettai, H., Oja, V., Freiberg, A., Laisk, A., 2005. Photosynthetic activity of far-red light in green plants. Biochim. Biophys. Acta 1708 (3), 311–321.
Schmidt, S.B., Jensen, P.E., Husted, S., 2016. Manganese deficiency in plants: the impact on photosystem II. Trends Plant Sci. 21 (7), 622–632.
Schöttler, M.A., Kirchhoff, H., Weis, E., 2004. The role of plastocyanin in the adjustment of the photosynthetic electron transport to the carbon metabolism in tobacco. Plant Physiol. 136 (4), 4265–4274.
Schreiber, U., 2017. Redox changes of ferredoxin, P700, and plastocyanin measured simultaneously in intact leaves. Photosynth. Res. 134, 343–360.
Schreiber, U., Klughammer, C., 2016. Analysis of photosystem I donor and acceptor sides with a new type of online-deconvoluting kinetic LED-array spectrophotometer. Plant Cell Physiol. 57 (7), 1454–1467.
Sétif, P., Boussac, A., Krieger-Liszkay, A., 2019. Near-infrared *in vitro* measurements of photosystem I cofactors and electron-transfer partners with a recently developed spectrophotometer. Photosynth. Res. 142 (3), 307–319.
Shen, J.R., 2015. The structure of photosystem II and the mechanism of water oxidation in photosynthesis. Annu. Rev. Plant Biol. 66, 23–48.
Shimakawa, G., Ishizaki, K., Tsukamoto, S., Tanaka, M., Sejima, T., Miyake, C., 2017. The liverwort, Marchantia, drives alternative electron flow using a flavodiiron protein to protect PSI. Plant Physiol. 173 (3), 1636–1647.
Shimakawa, G., Sétif, P., Krieger-Liszkay, A., 2020. Near-infrared *in vivo* measurements of photosystem I and its lumenal electron donors with a recently developed spectrophotometer. Photosynth. Res. 144 (1), 63–72.
Steinbeck, J., Ross, I.L., Rothnagel, R., Gäbelein, P., Schulze, S., Giles, N., et al., 2018. Structure of a PSI–LHCI–cyt b6f supercomplex in Chlamydomonas reinhardtii promoting cyclic electron flow under anaerobic conditions. Proc. Natl. Acad. Sci. USA 115 (41), 10517–10522.
Sunil, B., Saini, D., Bapatla, R.B., Aswani, V., Raghavendra, A.S., 2019. Photorespiration is complemented by cyclic electron flow and the alternative oxidase pathway to optimize photosynthesis and protect against abiotic stress. Photosynth. Res. 139 (1–3), 67–79.
Takahashi, H., 2022. Cyclic electron flow A to Z. J. Plant Res. 135 (4), 539–541.